Proceedings of the IASS 2024 Symposium
Redefining the Art of Structural Design
August 26-30, 2024, Zurich Switzerland
Philippe Block, Giulia Boller, Catherine DeWolf,
Jacqueline Pauli, Walter Kaufmann (eds.)

Efficient structural design of reconfigurable spatial structures by adopting aerodynamic shapes

Stefanos GKATZOGIANNIS*, Marios C. PHOCAS,
Eftychios G. CHRISTOFOROU[a], Charis J. GANTES[b]

* Department of Architecture, University of Cyprus
75 Kallipoleos St., 1678 Nicosia, Cyprus
sgkatz01@ucy.ac.cy
[a] Department of Mechanical and Manufacturing Engineering, University of Cyprus
75 Kallipoleos St., 1678 Nicosia, Cyprus
[b] Institute of Steel Structures, School of Civil Engineering, National Technical University of Athens
9 Heroon Polytechniou St., Zografou, 15780 Athens, Greece

Abstract

Reconfigurable, temporary structures are associated with a wide range of applications in architecture. However, their practical feasibility is restricted by, amongst others, the lack of suitable design codes for their structural design. Existing structural design codes for fixed-shape structures comprise currently the only tool available in practice towards the safe design of reconfigurable, temporary structures as well. However, in most cases of temporary, lightweight structures where wind actions are predominant, the adaptive reconfiguration of the structure to an aerodynamic shape can alternatively lead to a reduction of internal forces and displacements, when higher wind speeds are evident. Therewith, the adoption of smaller cross-sections and by extension a more efficient structural design can be achieved. Such a possibility is explored in the present study. The structural response against wind actions of an axisymmetric temporary, reconfigurable spatial structure in two basic shapes, i.e., reconfigurations approximating a paraboloid's and an ellipsoid's geometry, is investigated and compared with that of a third reconfiguration, having aerodynamic shape. FEA are carried out to this end, while the wind actions are modelled as equivalent static loads. The comparative study provides an estimate of the possible gains obtained through reconfiguration of the structure and highlights further elaborate numerical analyses required.

Keywords: Reconfigurable spatial structures, reconfiguration shapes, structural design, adaptive architecture.

1. Introduction

Reconfigurable, temporary structures have gained significant attention in architectural discourse, due to their potential for versatile, smart applications [1]-[6]. These structures, characterized by adaptability, can offer solutions to a spectrum of architectural and engineering challenges, for a wide range of buildings, from expo and conference pavilions to disaster relief shelters. Their widespread adoption though, is hindered by the absence of specialized design codes tailored to their unique characteristics, see relevant discussion in Gkatzogiannis et al. [7]. Existing structural design codes, formulated for fixed-shape structures, are usually instead deployed for designing their reconfigurable counterparts. The structural engineer has to handle the task of deviating from the serviceability limits of the conventional codes when designing temporary structures, see Koumar et al. [8] and De Temmerman [9], as their strict use often results in suboptimal designs, which adopt larger cross-sections to mitigate displacements within acceptable limits. At the same time, the structural integrity remains of utmost importance.

Consequently, the efficiency of structural design for the case of reconfigurable structures is compromised, particularly in scenarios dominated by wind actions.

The structural response of spatial structures under wind actions though, is significantly influenced by their geometry, which affects their aerodynamic and structural efficiency, stiffness, external and internal pressure distribution, and susceptibility to wind-induced vibrations. Streamlined shapes, such as domes and curved surfaces, reduce wind resistance and drag, allowing smoother airflow and minimizing turbulent wake regions, while efficient force distribution can be achieved through suitable geometries like triangular and hexagonal grids, which achieve even load distribution and provide load path redundancy, enhancing robustness. Additionally, certain geometries are deployed to avoid resonant vibrations and increase stiffness, as seen in geodesic domes and space frames, while smooth, continuous shapes further enhance performance by minimizing wind shadow effects and vortex shedding. Examples of effective geometries include geodesic domes, arched roofs, and thin shell structures, all of which efficiently distribute stress and resist wind loads, ensuring safety and durability.

The present study aims to assess the feasibility of achieving a more efficient structural design against predominant wind actions through appropriate geometric reconfiguration of the structure, based on straightforward engineering assumptions and by implementing Finite-Element (FE) analyses. To this end, the structural response of a configuration of the investigated structure that resembles a half-teardrop against wind loads is compared to the spatial structure's two principal axisymmetric configurations of circular plan: a half-paraboloid and a half-ellipsoid. Hereinafter, the former is called teardrop and the latter two, paraboloid and ellipsoid respectively, for the sake of simplicity. The teardrop configuration is considered as it is initially expected, based on common engineering knowledge, to achieve significant increase in drag and minimization of stress peaks on the exposed surface. Structural design to Eurocodes for all relevant actions for the latter two configurations, which are coinvestigated as they satisfy basic architectural requirements, has already been investigated in [7], where initial expectations about the predominance of wind actions for the structural design were confirmed. Critical to the current inquiry is the exploration of various configurations as a means of minimizing internal forces, displacements and support reactions under wind loading. In summary, this paper presents a first-step systematic investigation into the structural behaviour of reconfigurable, temporary spatial structures, aiming to elucidate ways for enhancing their structural efficiency by exploiting their reconfigurable nature.

2. Case study

2.1. Application scenario

The current investigation focuses on the wind performance of a temporary and adaptable research pavilion tailored to specific architectural criteria. This pavilion is tasked with enabling safe and efficient deployment, reconfiguration and disassembly by a small team of users. Furthermore, it must withstand varied climatic and seismic conditions to ensure its versatility, with Greece serving as the designated location due to its heightened mean wind speeds and seismic activity. To accurately gauge the structural demands of the pavilion, the study employs stochastic methods to estimate design loads, adhering to Eurocode guidelines. Conservative values were deliberately selected for certain parameters during the structural design to enable safe deployment to several locations independently of the local climate. Less conservative values based on engineering judgement were adopted for some of the design parameters - a thorough documentation is presented by Gkatzogiannis et al. [7] - to prevent undesired increases in cross-section sizes and preserve the pavilion's deployable nature. The predominance of wind actions as design loads was confirmed, with loads from snow being also indicated as critical. The decision to focus on Greece as the application setting facilitates broader applicability across other European regions with less severe climatic and seismic conditions. Consequently, the findings of this study hold relevance beyond Greece, offering valuable insights into the design of reconfigurable structures across diverse deployment locations.

2.1. Reconfigurable structure

The investigated reconfigurable bearing structure is designed as a lightweight system comprising a central actuated telescopic pillar and eight sets of linkage bars. Each bar, measuring 1.0 meter in length,

is evenly distributed and arranged radially around the central pillar. The conceptualization of this structure is inspired by the vertical effective crank-slider approach as discussed in Phocas et al. [2]. During the initial stages of conceptual design, a thorough analysis determined that a reconfiguration of 16 bars on each diameter axis, with 8 bars on each side of the central pillar, would optimize the structure's transformability attributes. The diameter of the structure is fixed at 12 m. The reconfigurable bar linkage system, which is repeated axisymmetrically to comprise the 3D structure is illustrated in Figure 1.

The bars are assigned a CHS (Circular Hollow Section) 219.1 x 10.0 cross-section, adhering to EN 10210-2:2019 [10]. To enhance stability against horizontal loads, secondary bars with a CHS 101.6 x 6.0 cross-section, also conforming to EN 10210-2:2019 [10], interconnect the bar linkages in an axisymmetric pattern. All structural members of the bearing system are constructed from structural aluminium EN AW 6061, following EN 573-3:2019 [11], to maximize lightweight characteristics and minimize the need for corrosion protection measures. To ease deployment, the weight of each individual bar is limited to 18 kg, totalling 28 kg, when the weight of reconfigurable nodes on either side of the bar is considered. Moreover, to enhance adaptability and maintain the structure's lightweight nature, a THV membrane, supported on auxiliary metallic mechanisms designed to accommodate reconfigurations without compromising the membrane's structural integrity or tension, is proposed for the building's envelope.

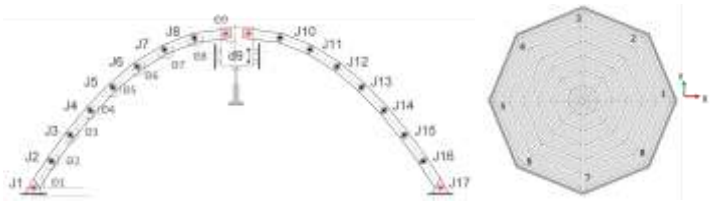

Figure 1: Planar section of the vertical effective crank–slider concept (left),
bar linkage numbering on the structure's plan (right)

The architectural demands of the structure necessitate multiple reconfigurations. A shape approximating the teardrop that satisfies the same architectural requirements as the paraboloid was also selected for the comparative investigation. Exact dimensions of the investigated shapes are defined by the reconfiguration compatibility and the architectural requirements through an architectural parametric investigation, which is presented by Irodotou et al. [12] for the axisymmetric shapes included in the present study, while the reconfiguration compatibility of the currently investigated teardrop shape was validated by similar analyses. Hence, the structural performance of the teardrop configuration under wind actions is compared in the present study with that of the paraboloid and quasi-ellipsoid. All three configurations are defined by the internal joint angles of each linkage, due to all bars having common length, as aforementioned. The internal angles are given in clockwise order in Table 1, while the three investigated configurations are illustrated in Figure 2. The height of each configuration is respectively 4.808, 3.153 and 3.972 m.

Table 1: Internal angles of the linkage bar systems for the investigated configurations, given in degrees

Shape	Bar linkage	Θ_1	Θ_2	Θ_3	Θ_4	Θ_5	Θ_6	Θ_7	Θ_8	Θ_9
Paraboloid	1-8	69.2	179.8	175.2	175.5	174.1	172.0	169.2	166.3	82.5
Ellipsoid	1-8	97.0	154.9	134.7	171.0	174.6	175.8	176.5	176.9	88.5
Teardrop	1	66.7	151.2	180.0	173.6	171.4	160.4	166.9	174.2	89.5
	2, 8	72.0	165.9	171.9	173.3	171.2	160.5	167.1	172.8	88.9
	3, 7	85.2	152.6	166.6	170.5	172.9	166.4	171.2	179.7	85.0
	4, 6	89.1	151.4	160.3	167.1	175.5	172.0	177.5	174.7	88.9
	5	92.8	154.4	160.0	166.8	175.1	172.1	177.8	171.4	89.5

Figure 2: The investigated configurations: the paraboloid (left), the ellipsoid (middle) and the teardrop (right)

2.3. Wind actions according to Eurocodes

2.1.1. Design values of wind pressure

In the framework of the present study, wind actions are evaluated according to the drafts of the new, upcoming generation of Eurocodes. More specifically, design values of wind pressures are obtained according to prEN 1991-1-4:2024 [13], according to which, the peak wind velocity $v_p(z)$ and the peak wind pressure $q_p(z)$, are composed of a mean and a fluctuating component. The mean wind velocity depends on the wind climate and the height variation of the wind determined from the terrain roughness and orography. The fluctuating component of the wind is represented by the turbulence intensity, $I_u(z)$.

The basic wind velocity, v_b, was calculated as follows:

$$v_b = c_{prob} \cdot c_{dir} \cdot c_{season} \cdot c_{alt} \cdot v_{b,0}, \tag{1}$$

where $v_{b,0}$ is the fundamental value of the basic wind velocity, taken equal to 33 m/s, that being the less favourable value from the most recent Greek wind map suggested by Malakatas [14], and c_{prob}, c_{dir}, c_{season} and c_{alt} are the probability, roughness, season and altitude factors, all taken equal to 1 as recommended by prEN 1991-1-4:2024 [13].

Based upon, the mean wind velocity, $v_m(z)$, was calculated as follows:

$$v_m(z) = c_r(z) \cdot c_o(z) \cdot v_b, \tag{2}$$

where $c_r(z)$ and $c_o(z)$ are the roughness and orography factor. $c_r(z)$ is a function of the structure's height, z, so it has distinct values for each configuration, being equal to 1.15, 1.09 and 1.21 for the paraboloid, ellipsoid and teardrop shapes, respectively. The less favourable value of the orography factor $c_o(z)$, equal to 1.48, was adopted to enable deployment of the investigated structure to all terrains. Turbulent intensity, is then calculated by Eq. (3):

$$\begin{gathered} I_u(z) = \frac{k_I}{c_0(z) \cdot \ln\left(\frac{z}{z_0}\right)}, \text{ for } z_{min} \le z \le z_{max}, \\ I_u(z) = I_u(z_{min}), \text{ for } z \le z_{min}. \end{gathered} \tag{3}$$

As orography influence was considered significant, peak velocity pressure, $q_p(z)$, was calculated as follows:

$$q_p(z) = \frac{1}{2} \cdot \rho_{wind} \cdot v_p^2\,(z), \tag{4}$$

where ρ_{wind} is the density of air taken equal to 1.25 kg/m^3 as recommended by prEN1991-1-4:2024 and

$$v_p(z) = v_m(z) \cdot (1 + k_u \cdot I_u(z)). \tag{5}$$

Finally, the spatial distributions of external wind pressures, w_e, were calculated based on Eq. (6):

$$w_e = q_p(z_e) \cdot c_{pe}, \tag{6}$$

where z_e, is the reference height for external pressure and c_{pe}, is the external pressure coefficient, which defines the spatial distribution of pressure on the 3D surface of the structure, as a function of its shape and the location of each point on the surface.

2.1.1. Spatial distribution of wind pressures

prEN1991-1-4:2024 provides c_{pe} distributions for common structures of symmetrical plans. Both the paraboloid and the ellipsoid were considered as domes of circular base for the needs of the present investigation with $h = 0$ and $f = h_{parboloid}$ for the former and $h = 1.943$ m and $f = h_{ellipsoid} - 1.943$ m$= 3.153$ m for the latter, where h and f are the total and the dome heights of the structure.

However, no relevant information is found in prEN1991-1-4:2024 [13], or in relevant literature known to the authors that could be of use in the case of the teardrop configuration. To tackle this, the following straightforward engineering approach was adopted for the present, first-step investigation, to enable a conservative comparison between the aerodynamic behaviour of the 3 configurations. The 3D surface of the teardrop structure, was modelled as a 3D point cloud in MATLAB [15] and was sliced along X axis (wind direction) into consecutive curves with 1 m distance between each other and with each one resembling the contour of an airfoil of different profile shape and dimensions. The airfoils are considered to be parallel to the wind at all times due to respective reconfiguration of the structure. Theoretical pressure distribution on upper parts of a typical airfoil, normalized to the peak velocity pressure (stagnation pressure) $1/2 \cdot \rho_{air} \cdot v^2$, found in Avallone and Baumeister [16] and illustrated in Figure 3, were adopted in order to estimate the qualitative air pressure distribution along each 2D slice of the 3D surface.

Nonetheless, these theoretical profiles are referring to airfoils in the scale of airplane wings and tend to produce pressure distributions, which are quantitatively unrealistic for significantly larger building structures according to common engineering knowledge. This is becoming evident, when the values of the theoretical c_{pe} distributions for the typical airfoil (Figure 3,) are compared to the c_{pe} distributions of the paraboloid and ellipsoid configurations of the structure, which were estimated to prEN1991-1-4:2024 and are presented in Figure 4, left and middle. To tackle this issue the c_{pe} theoretical distribution of the airfoils are normalized to their absolute peak value so that their suction (negative) peak value becomes -1, as in the case of the paraboloid's c_{pe} spatial distribution (Figure 4). This is considered a safe approximation, at least for the present preliminary study, as the projection of the two shapes opposing the incoming wind, resembles each other.

Subsequently, the values from the points on the 2D slices were interpolated on the rest points of the 3D surface mesh. The interpolated spatial estimated c_{pe} distributions on all points of the teardrop shape are included in Figure 4 (right). The numerical interpolation was completed for the nodes of the 3D surface between the outer two slices, i.e. for Y coordinate ranging inside [-5, 5] which can be seen in Figure 4, while for the outer parts of the 3D surface, a linear distribution considering $c_{pe} = 0$ at height $Z = 0$ was considered in the FE simulation mode.

It has to be further noted, that the adopted c_{pe} distributions for the teardrop shape are, at least qualitatively conservative, as they neglect inwards pressure, which is known to develop at the base and around the centre of the structure's projection facing the wind, (also evident for the other two configurations) and assume pure suction (outwards pressure) all along the outer surface of the shape. The conservatism is obvious when the equilibrium of the structure is considered, as in a different case the inwards pressure would balance a fraction of the suction force and hence, lower uplift reaction forces would be estimated. However, even in the case of action effects arising in the bearing system, overall conservative results are expected with regard to tension and bending, due to once again neglection of the pressure component counterbalancing suction. On the contrary, the adoption of wind pressures neglecting inwards pressure could lead to non-conservative results, in the case when superposition with significant vertical loads (e.g., snow actions) takes places, as it could lead to overseeing local overstress. Such an interpretation however is beyond the scope of this first-step investigation and will be addressed in future work.

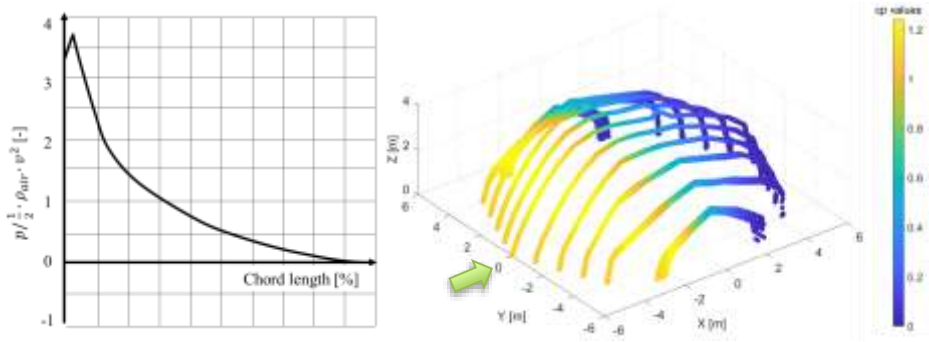

Figure 3: Theoretical fluid pressure distribution p/q_p on the upper side of a typical airfoil (left) and extrapolated pressure distributions on each slice of the teardrop's surface (right) – the green arrow indicates the wind direction

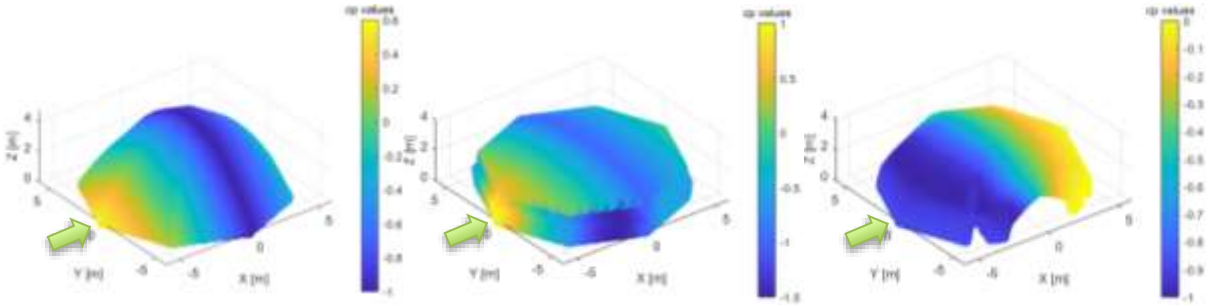

Figure 4: c_{pe} distributions for the paraboloid (left), the ellipsoid (middle) and the teardrop (right) – the green arrows indicate the wind direction

2.3. Numerical model

For the present analyses, the commercial FE software RFEM [17] was utilized, employing linear FE models with beam elements to simulate the structure. The current modelling approach adopts a simplification by disregarding the building's envelope, under the rational assumption that its contribution to stiffness is negligible. Instead, the weight and loads of the envelope are transferred to the load-bearing members of the structure. The reconfigurable joints were modelled as continuous (moment-resisting), leading to a stiffer structure, which is expected to produce conservative results regarding stress resultants. Each bar linkage system consisting of 8 bars is treated as a single structural component, significantly increasing its considered buckling length. Pinned connections of the bar systems and the central pillar to the ground are modelled.

Two load cases were considered. The first one was denoted G and included all dead loads i.e. the self-weight of the structural components, the reconfigurable joint mechanism, considering conservatively a weight of 0.1 kN, and the self-weight of the membrane and its supporting mechanism. The second one was denoted W_x including the wind actions, for wind across the X axis. Consideration of a single wind direction is considered sufficient as the first two configurations are axisymmetric, while the teardrop shape is considered to be oriented with its longitudinal axis to the wind origin in the aerodynamically optimum configuration. The two load cases were super-positioned, without any multiplication factors, as this is considered unnecessary for the present comparative analysis, i.e. $G + W_x$ is modelled. Although not realistic, results of the wind actions W_x neglecting G are also presented bellow, to offer a clearer insight in the structural response of the investigated configurations to wind actions. Static Linear Analyses (LA) were carried out as for the present load combination, while 2nd order phenomena are expected to be negligible. The following material properties were adopted: Modulus of elasticity $E = 70$ GPa, poisson's ratio $\nu = 0.296$ and proof strength $f_0 = 110$ MPa.

3. Results and discussion

The von Mises stress distribution, extracted by the conducted analyses for the load case W_x and the load combination $G + W_x$ are presented in Figure 5 for the three investigated configurations. It should be

elaborated, that beyond the internal forces in the bearing members, the reactions at the supports and uplift forces are also important for the deployable character of the structure, as these affect the conception of the deployable foundation mechanisms that should accompany the upper aluminium structure. Hence, they are also presented bellow and are considered in the evaluation of the investigated shapes' structural performance against wind actions.

Comparing the stress distributions of the three configurations, a negligible reduction of the utilization factor is achieved, when the teardrop configuration is compared with the paraboloid configuration. The peak von Mises stress are estimated at 47 MPa and 46 MPa for the former one and for the cases W_x and $G + W_x$, against 48 MPa for both load cases, for the latter one. On the contrary, the ellipsoid configuration seems to be more efficient in terms of aerodynamic performance, with peak von Mises stress of 40 and 37 MPa respectively. The improved performance of the ellipsoid configuration is attributed mainly to the reduction of the structure's height.

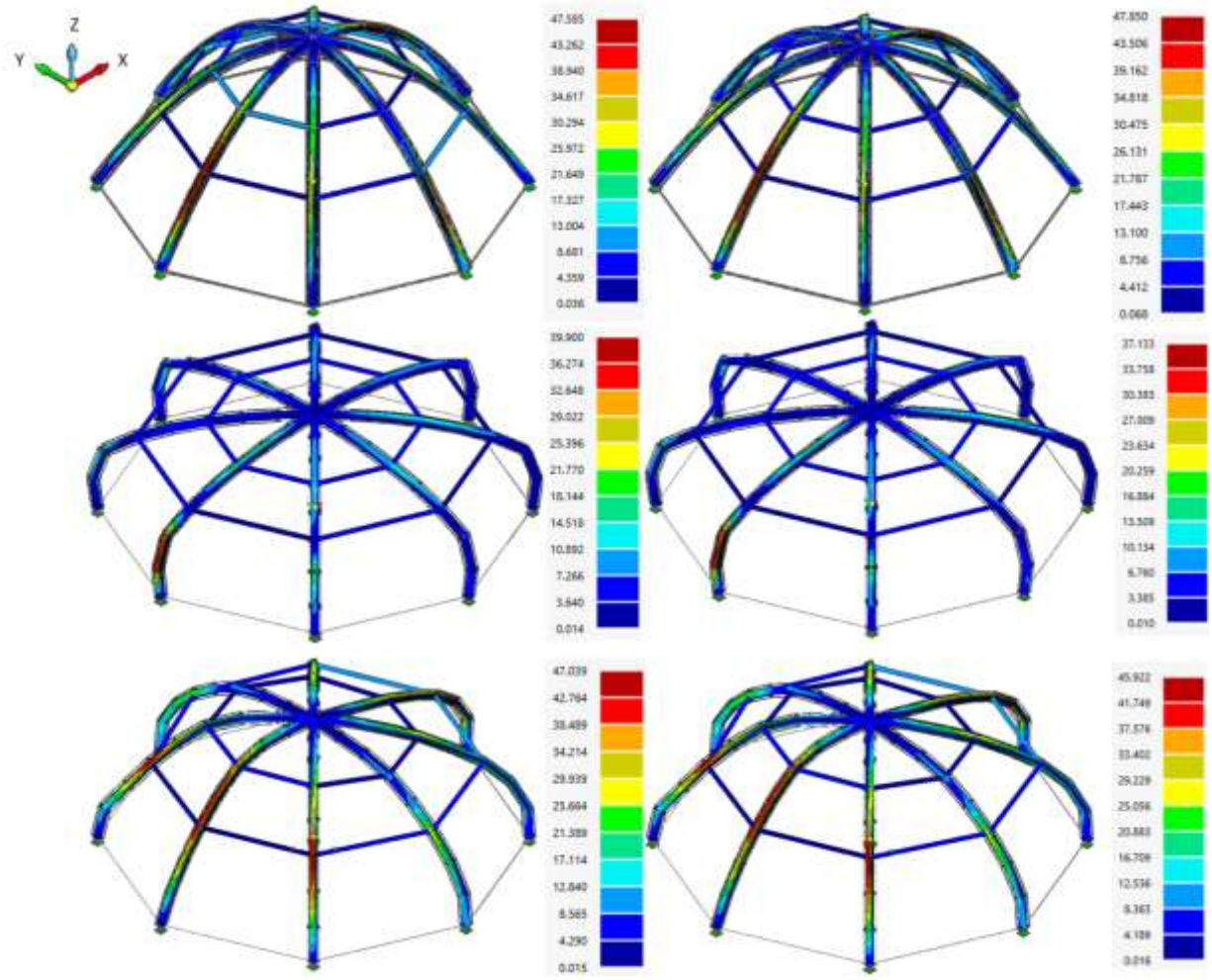

Figure 5: von Mises stress distribution for the actions W_x (left) and $G + W_x$ (right)
isometric views of the paraboloid (top), ellipsoid (middle) and teardrop (bottom) configurations

Similarly, superior behaviour of the ellipsoid is concluded, when the documented peak absolute value of the reactions at the supports $[P_x, P_y, P_z]$, the peak uplift force at the supports, the sum of the loads/support reactions and the maximum displacements $[u_x, u_y, u_z, u]$, which are presented in Table 2, are considered. Once again, lower support reactions, sum of forces and displacements are documented for the ellipsoid shape, highlighting its improved structural response against wind actions in comparison to that of the other two configurations. Nevertheless, this time a non-negligible deviation in the performance of the two other configurations is met, with significant reduction of the reactions at the

supports and the sum of the loads being documented for the teardrop shape, while lower displacements and peak uplift force at the supports are documented for the paraboloid configuration.

It is becoming evident from the above, that reconfiguration of a structure can be applied as a means of improving its structural response against wind actions significantly, altering structural utilization and need for counterbalance of uplift forces. It should be underlined that significantly higher utilization was documented for the ellipsoid in [7], when wind and snow loads were superimposed in comparison to the paraboloid configuration, despite its superior structural behaviour against wind actions documented here. Hence, the present results should be applied with caution and for selecting shapes to further investigate and are not a direct indicator of the optimum configuration for loading scenarios superimposing all relevant actions, despite wind loads being predominant. Moreover, as it was elaborated above, the estimation of the equivalent static loads for the teardrop configuration is conducted based on a rough estimation considering theoretical pressure distribution for airfoils of smaller scale. Scale effects are considered in a practical way, however this approximation may be inaccurate. Although the adopted assumptions are expected to act conservatively, as already discussed above, still this has to be proven by further more elaborate analysis.

Table 2: Results of the linear analysis for the 3 configurations for the combination $G + W_x$

	Configuration	Paraboloid	Ellipsoid	Teardrop
W	support reactions $[P_x, P_y, P_z]$ in kN	[13.6, 16.8, 44.6]	[14.8, 8.4, 19.6]	[10, 3.5, 17.9]
	uplift force in kN	9.4	0	14.27
	sum of loads in kN	[42.2, -2.7, 144.7]	[22.9, -0.47, 129.8]	[37.8, 4.4, 75.9]
	max displacements $[u_x, u_y, u_z, u]$ in mm	[34.8, -6.9, -25.2, 43]	[7.9, -4.0, 6.5, 9.1]	[42.7, 3.4, 23.5, 47.7]
G+W	support reactions $[P_x, P_y, P_z]$ in kN	[12.5, 15.2, 41.9]	[14.2, 8.9, 17.5]	[9.1, 3.0, 17.5]
	uplift force in kN	10.3	0	17.5
	sum of loads in kN	[42.2, -2.7, 123.4]	[22.9, -0.47, 108.4]	[37.8, -4.4, 55.2]
	max displacements $[u_x, u_y, u_z, u]$ in mm	[34.8, -6.9, -25.2, 43.1]	[7.7, -4.0, 5.7, 8.6]	[42.6, 3.6, 23.3, 47.9]

4. Conclusions and future work

Based on the above, it is concluded that a reconfiguration to a different shape can improve the wind performance of the structure and lead to more efficient design. Among the investigated configurations, the ellipsoid configuration enables superior structural performance against wind actions. It should be noted however, that the ellipsoid configuration serves different architectural needs than the paraboloid. The teardrop configuration on the contrary, having comparable height and building plan with the latter one, can satisfy the same requirements but its structural response against wind actions still deviates from that of the paraboloid. Hence, even with a negligible modification of the structure's shape in terms of architectural functionality, the wind performance of the buildings changes significantly, and when specific aspects are considered, it can be optimized. More elaborate numerical analysis implementing CFD (Computational Fluid Dynamics) are already planned in future work of the authors, in order to validate the conservatism of the adopted, straightforward assumptions and further check the aerodynamic behaviour of the investigated shapes.

Acknowledgements

The authors would like to acknowledge the ONISILOS and MSCA COFUND (Marie Skłodowska-Curie Grant Agreement No 101034403) for financing the research project DY.R.E.B., in the framework of which the present study was conducted.

References

[1] M. C. Phocas, E. G. Christoforou, M. Matheou and N. Georgiou, "Kinematics Approach and Experimental Verification of a Class of Deployable and Reconfigurable Linkage Structures," *Structural Engineering*, vol. 150, no. 1, pp. 04023206/1-14, 2024.

[2] M. C. Phocas, E. G. Christoforou, C. Theokli and K. Petrou, "Reconfigurable Linkage Structures and Photovoltaics Integration," *Building Engineering*, vol. 43, pp. 103201/1-12, 2021.

[3] M. C. Phocas, N. Georgiou and E. C. Christoforou, "A Class of Actuated Deployable and Reconfigurable Multilink Structures," *Advances in Computational Design*, vol. 7, no. 3, pp. 189-210, 2022.

[4] M. C. Phocas, M. Matheou and W. Haase "Transformable Building Structures in Architectural Engineering Education," *Architecture, Structures and Construction*, vol. 2, pp. 183-198, 2022.

[5] M. C. Phocas, M. Matheou, M. Müller and E. C. Christoforou, "Reconfigurable Modular Bar Structure," *Journal of the International Association for Shel and Spatial Structures*, vol. 60, no. 1, pp. 78-89, 2019.

[6] C. J. Gantes, "*Deployable Structures - Analysis and Design*, " WIT Press, 2001.

[7] S. Gkatzogiannis, M. C. Phocas and E. C. Christoforou, "Structural Design of a Reconfigurable and Temporary Spatial Structure According to the Eurocodes," abstract accepted / full paper under review, to be presented in *ACEM24 - The World Congress 2024 on Advances in Civil, Environmental, and Materials Research*, Seoul 19–22 August, 2024.

[8] A. Koumar, T. Tysmans and N. De Temmerman, "Structural Design of Barrel Vault Shaped Scissor Structures for Disaster Relierf," *Journal of the International Association for Shell and Spatial Structures*, vol. 59, no. 3, pp. 171-182, 1995.

[9] N. De Temmerman, "Design and Analysis of Deployable Bar Structures for Mobile Architectural Applications," Ph.D. Thesis, Vrije Universiteit Brussel, 2007.

[10] EN 10210-2:2019, "Hot Finished Steel Structural Hollow Sections - Part 2: Tolerances, Dimensions and Sectional Properties."

[11] EN 573-3:2019+A2:2023, "Aluminium and Aluminium Alloys – Chemical Composition and Form of Wrought Products – Chemical Composition and Form of Products."

[12] L. Irodotou, S. Gkatzogiannis, M. C. Phocas, G. Tryfonos and E. G. Christoforou, "Application of a Vertical Effective Crank–Slider Approach in Reconfigurable Buildings through Computer-Aided Algorithmic Modelling," abstract accepted / full paper under review, to be presented in *eCAADe – Education and Research in Computer Aided Architectural Design in Europe,* Nicosia 9 –10 September, 2024.

[13] prEN 1991-1-4:2024, "Actions on Structures – General Actions – Wind Actions."

[14] N. Malakatas, "EN 1991 – Climatic Actions & Elaboration of Maps for Climatic Actions in Greece," *Elaboration of Maps for Climatic and Seismic Actions for Structural Design in the Balkan Region*, Zagreb, 27-28 October 2015.

[15] "MATLAB and Statistics Toolbox," The MathWorks, Natick, Massachusetts, USA, 2023.

[16] E. A. Avallone and T. Baumeister III (eds), *Marks' Standard Handbook for Mechanical Engineers*, 10th Edition, McGraw-Hill, 1996.

[17] "Dlubal RFEM 6: Software for Structural Analysis," Academic license, Dlubal Software GmbH, Tiefenbach, Germany, 2024.